Neuron, Vol. 17, 695–706, October, 1996, Copyright ©1996 by Cell Press

A Putative Cyclic Nucleotide–Gated Channel Is Required for Sensory Development and Function in C. elegans

Cara M. Coburn and Cornelia I. Bargmann
Howard Hughes Medical Institute
Programs in Developmental Biology, Neuroscience, and Genetics
Department of Anatomy
The University of California
San Francisco, California 94143-0452

Summary

In vertebrate visual and olfactory systems, a cyclic nucleotide–gated channel couples receptor activation to electrical activity of the sensory neurons. The Caenorhabditis elegans *tax-2* gene is required for some forms of olfaction, for chemosensation of salts, and for thermosensation. We show here that *tax-2* encodes a predicted subunit of a cyclic nucleotide–gated channel that is expressed in olfactory, gustatory, and thermosensory neurons, implicating this channel in multiple sensory modalities. Some sensory neurons display axon outgrowth defects in *tax-2* mutants. Thus, the channel has an unexpected role in sensory neuron development in addition to its role in sensation. Consistent with this proposed dual function, a Tax-2::GFP fusion protein is present both in sensory cilia and in sensory axons.

Introduction

Sensory neurons respond to the environment by transducing external stimuli into patterned electrical activity. In both vertebrate visual and olfactory neurons, sensory receptor proteins initiate this process by regulating second messengers that open cyclic nucleotide–gated ion channels. In photoreceptors, light-activated rhodopsin stimulates cGMP hydrolysis to reduce channel activity; in olfactory neurons, odorants induce cAMP production to stimulate channel activity (Fesenko et al., 1985; Sklar et al., 1986; Nakamura and Gold, 1987; Stryer, 1991). Although they are regulated by different nucleotides, the genes that encode vertebrate visual and olfactory cyclic nucleotide–gated channels are similar to one another (Kaupp et al., 1989; Dhallan et al., 1990; Bonigk et al., 1993).

The cyclic nucleotide–gated channels are distantly related to the Shaker class of voltage-gated potassium channels, but they are gated by an intracellular ligand (cAMP or cGMP) instead of membrane potential. Cyclic nucleotide binding to an intracellular domain of the channel allows nonspecific cation entry and neuronal depolarization (Goulding et al., 1994). Each channel is composed of related α and β subunits that assemble to form a heteromeric channel protein (Chen et al., 1993; Bradley et al., 1994; Liman and Buck, 1994; Korschen et al., 1995).

Although the prominence of cyclic nucleotide–gated channels in sensory transduction is well established, questions about their function remain. First, other types of odor-activated channels have been reported in olfactory neurons, and the relative importance of each channel in signal transduction is unknown (Kleene, 1993; Lowe and Gold, 1993; Dubin and Dionne, 1994). Second, it is not known whether the cyclic nucleotide–gated channels in sensory neurons act only in sensory transduction, or if they participate in other aspects of neuronal function. Third, these channels are expressed in other neuronal and non-neuronal cell types, but their function in these cell types is not understood (Ahmad et al., 1994; Biel et al., 1994; Weyand et al., 1994; el-Husseini et al., 1995).

In Caenorhabditis elegans, genetic analysis can be used to probe chemosensory transduction in vivo. The C. elegans nervous system contains 32 chemosensory neurons, which can be divided into 14 types based on morphology (Ward et al., 1975; Ware et al., 1975; White et al., 1986). Laser killing experiments have demonstrated chemosensory functions for ten types of neurons in the major chemosensory organ, the amphid (Bargmann and Horvitz, 1991a, 1991b; Bargmann et al., 1993; Kaplan and Horvitz, 1993; Troemel et al., 1995). Different amphid neurons can detect water-soluble attractants, volatile attractants, pheromones, and chemical repellents. The amphid also contains one type of neuron that detects temperature (Mori and Ohshima, 1995). Screens for chemotaxis mutants in C. elegans have identified mutations in various *odr*, *che*, and *tax* genes (Dusenbery et al., 1975; Lewis and Hodgkin, 1977; Bargmann et al., 1993). Some of these mutants have defects in many chemosensory neurons, while others have defects that are limited to one or a few chemosensory responses.

Olfactory recognition in C. elegans appears to be initiated by interactions between odorants and G protein–coupled receptors. Genetic and molecular analysis suggests that a seven transmembrane domain protein encoded by the *odr-10* gene is a diacetyl receptor, although it has not been demonstrated to bind to odorant (Sengupta et al., 1996). *odr-10* is required for the response to the volatile odorant diacetyl, and a tagged Odr-10 protein is localized to the sensory cilia of the neurons that detect diacetyl. Several different families of predicted G protein–coupled receptors could encode additional C. elegans chemoreceptors. There are at least 40 candidate receptor genes in six gene families (the *sra, srb, srd, sre, srg,* and *sro* genes) that appear to be expressed predominantly in chemosensory neurons (Troemel et al., 1995), as well as at least 80 other *odr-10*-like genes (E. Troemel, J. Chou, and C. I. B., unpublished data). Each individual chemosensory neuron appears to express several different candidate chemosensory receptor genes (Troemel et al., 1995); correspondingly, laser killing experiments and behavioral studies indicate that each chemosensory neuron detects several chemical stimuli (Ward, 1973; Colbert and Bargmann, 1995).

The second messenger pathways that are used by C. elegans sensory neurons are not known. While the *odr-10* mutant phenotype is extremely selective, as is expected of a receptor, we expected that the genes that act in sensory transduction might affect multiple sensory

Table 1. *tax-2* Behavioral Defects Are Similar to the Loss of Some Amphid Neuron Functions

Amphid Neuron	Function	*tax-2 (p671,p691,ks10,ks15, ks31,ky139)* Phenotype	*tax-2(p694)* Phenotype
AWA	Pyrazine, diacetyl, trimethythiazole chemotaxis[a]	+	+
AWC	Benzaldehyde, isoamyl alcohol, 2-butanone, trimethythiazole chemotaxis[a]	−	+
AFD	Thermotaxis[b]	−[f]	−[f]
ASE	Chemotaxis to water-soluble compounds (NaCl)[c]	−[g] Axon morphology abnormal	−[g]
ASH	Osmotic avoidance; nose-touch avoidance[d]	+	+
ASJ	Regulation of dauer recovery[e]	Axon morphology abnormal	+
ASK	Lysine chemotaxis[c]	−	ND

All alleles were tested for volatile chemotaxis, NaCl water-soluble chemotaxis, ASJ axon morphology, and osmotic avoidance. Only *tax-2(p691)* was tested for ASE axon morphology and lysine chemotaxis. Published thermotaxis data for *p671*, *p691*, and *p694* are cited.
[a] Bargmann et al. (1993); [b] Mori and Ohshima (1995); [c] Bargmann and Horvitz (1991a); [d] Kaplan and Horvitz (1993); [e] Bargmann and Horvitz (1991b); [f] Hedgecock and Russell (1975); [g] Dusenbery et al. (1975). Abbreviations: ND, not determined.

responses. We describe here the characterization of the *tax-2* gene, which affects chemotaxis to attractive compounds, avoidance of repulsive compounds, and thermotaxis (Dusenbery et al., 1975; Hedgecock and Russell, 1975; Bargmann et al., 1993). *tax-2* encodes a predicted subunit of a cyclic nucleotide–gated channel. An additional cyclic nucleotide–gated channel subunit that might function with *tax-2* is encoded by the *tax-4* gene (Komatsu et al., 1996 [this issue of *Neuron*]); *tax-4* affects the same behavioral responses as does *tax-2*. *tax-2* is expressed in the subset of sensory neurons whose function is defective in the mutants.

In addition to their apparent sensory function, both *tax-2* and *tax-4* have an unexpected role in sensory axon guidance. In *tax-2* and *tax-4* mutants, sensory axons invade regions from which they are normally excluded, suggesting that channel activity inhibits or limits axon outgrowth of sensory neurons.

Results

tax-2 Encodes a Cyclic Nucleotide–Gated Channel Subunit Required for Multiple Sensory Functions

Seven *tax-2* mutant alleles have been isolated based on defects in chemotaxis, thermotaxis, and dauer larva formation (Dusenbery et al., 1975; C. M. C., I. Mori, Y. Ohshima, C. I. B., unpublished data). These mutants were compared with one another in various behavioral assays. All tested alleles were defective in chemotaxis to water-soluble attractants and in thermotaxis (Dusenbery et al., 1975; Hedgecock and Russell, 1975; Table 1); similar defects are associated with loss of function of the ASE, ASK, and AFD sensory neurons. In addition, six of the seven mutants were defective in chemotaxis to a subset of volatile odorants (Figure 1). *p671, p691, ks10, ks15, ks31,* and *ky139* were defective for chemotaxis to benzaldehyde and isoamyl alcohol, but proficient in chemotaxis to diacetyl, pyrazine, and trimethylthiazole. These chemotaxis defects are characteristic of animals that lack the function of the AWC olfactory neurons, but maintain function of the AWA olfactory neurons (Bargmann et al., 1993) (Table 1). By contrast, animals mutant for the *tax-2* allele *p694* were normal for chemotaxis to all volatile odorants.

Negative chemotaxis responses to volatile repellents including 1-octanol and 2-nonanone were also defective in *tax-2(p671), tax-2(p691),* and *tax-2(ks31)* mutants; the cells required for these responses are unknown. However, the mutants responded normally to water-soluble repellents, which are detected by the ASH sensory neurons. Movement, fertility, and development appeared

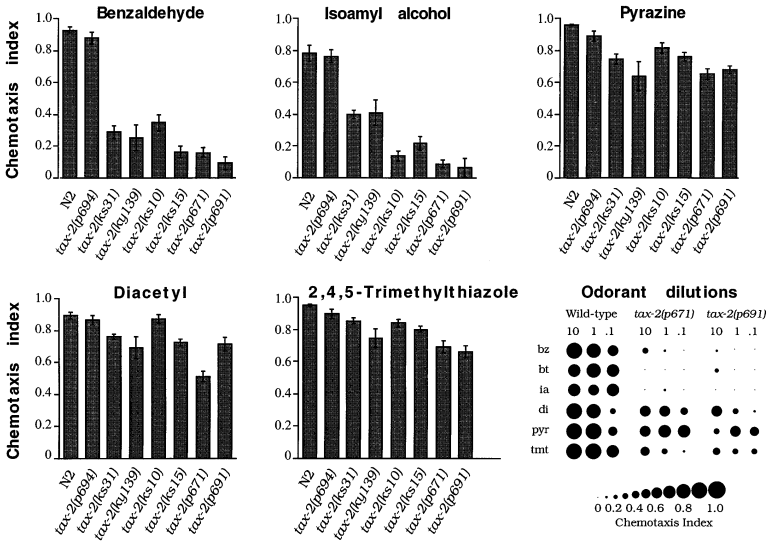

Figure 1. Responses of *tax-2* Mutants to Volatile Odorants

Each data point represents the average of at least eight independent assays using ~100–200 well fed adult animals per assay (error bars equal the SEM). The dilution of odorants in ethanol were the following: 1:200 benzaldehyde (bz), 1:100 isoamyl alcohol (ia), 10 mg/ml pyrazine (pyr), 1:1000 diacetyl (di), and 1:1000 2,4,5-trimethylthiazole (tmt). Selected alleles were also tested to a range of odorant dilutions at 10×, 1×, and 0.1× the standard odorant dilution (e.g., benzaldehyde was tested at 1:20, 1:200, and 1:2000). Butanone (bt), an AWC-sensed odorant, was tested at 1:100, 1:1000, and 1:10,000.

normal, though the mutants were often slightly smaller than wild-type animals and had slightly slowed development.

These results indicate that most *tax-2* alleles affect a common set of sensory functions, while the weak allele *p694* only affects a subset of those functions. All of the *tax-2* mutants are recessive and fail to complement one another. In addition, the phenotype of *tax-2(p691)* is not enhanced in a *tax-2(p691)*/deletion heterozygote (data not shown). Taken together, these results are consistent with the mutations causing a loss of *tax-2* gene function.

tax-2 was cloned by genetic mapping and cosmid rescue of *tax-2* mutants (Figure 2A). cDNA clones from the rescuing region were identified by screening a mixed-stage library and by reverse transcriptase–polymerase chain reaction amplification of *tax-2* clones from total mRNA. The genomic sequence and the sequence of cDNA clones representing the entire *tax-2* coding regions were determined.

tax-2 encodes a predicted protein of 800 amino acids with substantial structural and sequence similarity to the cyclic nucleotide–gated channels from vertebrate photoreceptors and olfactory neurons (Figure 2C). The overall structure consists of a nonconserved amino-terminal region, a central region that includes six potential membrane-spanning domains, and a carboxy-terminal cyclic nucleotide–binding domain (Henn et al., 1995). Based on the presence of an asparagine residue at position 662, *tax-2* would be predicted to interact more strongly with cGMP than with cAMP (Varnum et al., 1995). *tax-2* was most similar to the β subunit of the human rod channel, with which it shared 40% amino acid identity over the transmembrane domains and cyclic nucleotide–binding domain. *tax-2* and the β subunit of the rod channel were more similar to one another than either was to any other member of the channel family (Figure 2B).

To confirm the identification of the *tax-2* gene, the coding regions of the mutant alleles were sequenced. The weak allele *tax-2(p694)* was a deletion of the first exon and about 1.8 kb of upstream sequences (Figures 2A and 2C). Four of the other mutations were missense mutations in the potential membrane-spanning regions of *tax-2* (Figure 2C), including three mutations found within the predicted pore region. *tax-2(p691)* led to the substitution of a serine for a proline residue at position 426, *tax-2(ky139)* led to the substitution of a cysteine for an arginine residue at position 410, and *tax-2(ks31)* led to the substitution of an isoleucine for a threonine residue at position 427. *tax-2(p671)* was a missense mutation in the first membrane-spanning domain, leading to the substitution of an arginine for a cysteine at position 229. The presence of these mutations at conserved positions suggests that the predicted pore region and membrane-spanning domains are essential for normal *tax-2* function, consistent with the prediction that it acts as part of a channel.

The *tax-4* gene encodes a predicted subunit of a cyclic nucleotide–gated channel that is most similar to the α subunits of the vertebrate rod and olfactory channels (Komatsu et al., 1996). The phenotypes and expression patterns of *tax-2* and *tax-4* mutants are similar, suggesting that these two genes function in the same sensory neurons (see below).

tax-2 Is Expressed in Thermosensory Neurons and a Subset of Chemosensory Neurons

To ask whether *tax-2* functions within the sensory neurons or in the interneurons that mediate chemosensory behaviors, the expression of *tax-2* was examined. Fusions of *tax-2* to the green fluorescent protein (GFP) revealed expression of GFP in 11 classes of sensory neurons (Figure 3). *tax-2::GFP* expression was observed in all four types of neurons that were affected in *tax-2* mutants, including neurons required for thermotaxis, water-soluble chemotaxis, and volatile chemotaxis (AFD, ASE, ASK, and AWC). It was not expressed in sensory neurons whose function was intact in *tax-2* mutants, or in any nonsensory cell type.

The expression pattern suggests that *tax-2* acts cell-autonomously in the sensory cells whose function is compromised in these mutants. Support for this model is provided by analysis of the *tax-2* deletion mutation *p694,* which lacks the first exon and the upstream region of *tax-2.* A *tax-2Δ::GFP* fusion with a similar deletion was expressed in only seven classes of sensory neurons. The deleted fusion gene was expressed in the AWC neurons, whose function was normal in *p694* mutants, but not in the AFD or ASE neurons, whose function was disrupted by the *p694* deletion (Figure 3B). This correlation is consistent with a direct requirement for *tax-2* expression within the affected sensory cell types; it also indicates that *tax-2* defects are caused by a loss of gene function, at least in AFD and ASE.

Comparison of three *tax-2::GFP* fusion genes revealed two distinct regions that regulated *tax-2::GFP* expression in different neurons (see Figure 2A; Figure 3). An upstream element was required for expression in four cell types (ADE, AFD, ASE, BAG), while a region in the first intron was required for consistent expression in ASG, ASJ, ASK, and AWB. Either the upstream region or the first intron was sufficient for expression in ASI, AWC, and PQR.

To confirm these observations, two *tax-2* genomic clones were tested for rescue of different *tax-2* phenotypes (see Figure 2A). Only a clone that included the upstream element rescued Cl^- chemotaxis, consistent with the observation that the upstream element was required for ASE expression. However, a clone that lacked the first exon and upstream sequences could fully rescue benzaldehyde chemotaxis, consistent with the AWC expression of a similar *tax-2::GFP* fusion gene.

Interestingly, these results also indicate that the normal amino terminus of *tax-2* is not required for its olfactory function in AWC, since the first coding exon is deleted in *tax-2(p694)* and in the shorter *tax-2* rescuing fragment. The truncated *tax-2(p694)* protein might initiate at methionine 138 of *tax-2*, upstream of the first transmembrane domain. A short version of the rod β channel that lacks much of its nonconserved amino terminus retains normal channel function when expressed in Xenopus oocytes (Chen et al., 1993; Korschen et al., 1995).

tax-2 and *tax-4* Affect Axon Outgrowth of Some Sensory Neurons

All of the known defects in *tax-2* and *tax-4* mutants can be ascribed to defective function of the amphid

A

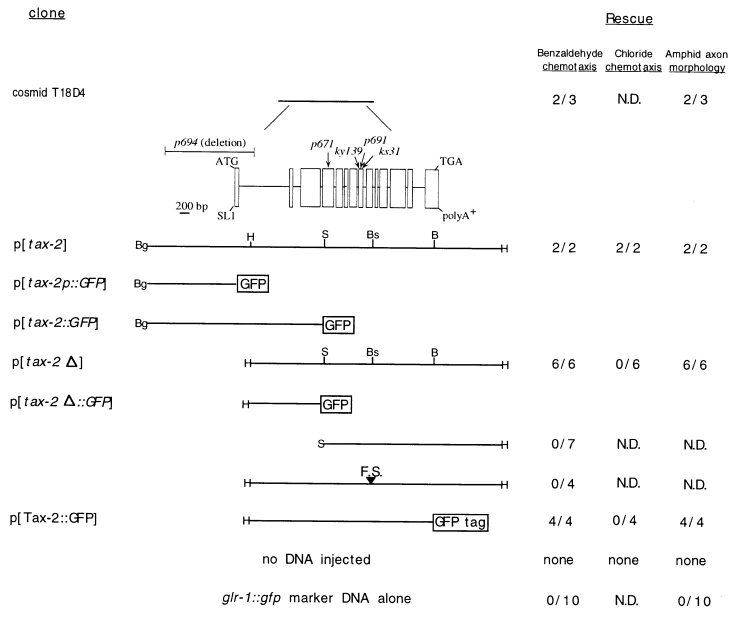

B

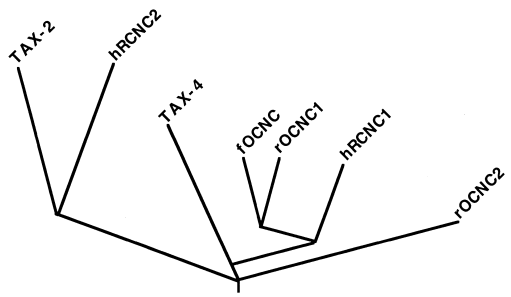

Figure 2. Localization and Sequence Analysis of *tax-2*

(A) Localization of the *tax-2* gene. Cosmid T18D4 and subclones were tested for rescue of the chemotaxis and amphid axon defects of *tax-2(p691)*. For each experiment, the number of independent transformed lines that rescued the *tax-2* mutant phenotype is given as a fraction of the total number of lines tested. Rescue was scored if a line had a chemotaxis index $\geq$0.6, or had >50% normal amphid axon morphology assessed by dye filling (this assay reveals ASJ axons but not ASE axons). Inset diagram shows *tax-2* genomic organization with the location of the *p694* deletion and the *p671*, *ky139*, *p691*, and *ks31* mutations indicated. Boxes depict exons. GFP expression plasmids are described in Experimental Procedures. An inverted triangle indicates the restriction site at which a frameshift mutation was created. Abbreviations: B, BamHI; Bg, BglII; Bs, BsaBI; H, HindIII; S, SalI.

(B) A rooted parsimonious tree of cyclic nucleotide–gated channel protein sequences from the first transmembrane domain through the cyclic nucleotide–binding site. Tree was calculated using the Phylogeny Inference Package of programs (Felsenfeld, 1989). Prefixes: h, human; r, rat; f, catfish.

(C) Predicted amino acid sequence of the *tax-2* cDNA and sequence comparisons. The comparison between the predicted amino acid sequences of the *tax-2* cDNA, the short form of the human rod cyclic nucleotide–gated channel β subunit (hRCNC2; Chen et al., 1993), and the rat olfactory cyclic nucleotide–gated channel α subunit (rOCNC1; Dhallan et al., 1990) is shown. Identical residues are shaded. Amino acids are numbered beginning at the first methionine. Predicted transmembrane domains and the cyclic nucleotide–binding domain are underlined. The location of the *p694* deletion and the *p671*, *ky139*, *p691*, and *ks31* mutations are indicated along with the predicted amino acid alterations. The predicted ATG used in the *p694* deletion mutant and in clone p[*tax-2Δ::GFP*] is marked by an asterisk.

(*Figure 2 continued on next page*)

chemosensory neurons. The amphids are a bilaterally symmetric pair of sensory organs in the head that each contain 12 sensory neurons; the phasmid organs of the tail each contain 2 sensory neurons (Ward et al., 1975; Ware et al., 1975). The sensory neurons are bipolar neurons, with one axon, or presynaptic process, and one dendrite, which terminates in the sensory cilia (Figure 3; Figure 4). The axons of the amphid neurons extend to a central neuropil called the nerve ring, in which they synapse onto target neurons. The phasmid axons synapse onto their targets in the ventral nerve cord neuropil.

Interestingly, defects in sensory axon development were observed in *tax-2* and *tax-4* mutants. The sensory neurons were examined using the dye DiO, which stains dendrites, cell bodies, and axons of six amphid neuron pairs and two phasmid neuron pairs (Herman and Hedgecock, 1990) (Figures 4A and 4D). The most common defect was the presence of one or more inappropriate posteriorly directed amphid axons in the ventral nerve cord (Figure 4B). The process was assigned to the ASJ neurons by examining different subsets of axons with GFP fusion genes (see Experimental Procedures).

In wild-type animals, the axons of the ASJ neurons terminate in the dorsal nerve ring. In 60%–90% of *tax-2* and *tax-4* mutants, at least one ASJ axon bypassed its normal site of termination and extended into the ventral nerve cord (Figure 5). Furthermore, in 5% of *tax-2* and *tax-4* mutants, the initial outgrowth of the ASJ axon was posteriorly, rather than ventrally, directed (see Figure 4C).

The six strong *tax-2* mutations showed comparable axon phenotypes, but the weak *tax-2* mutant *p694* did not display any ASJ developmental defects. In addition, both the full-length *tax-2* genomic clone and the clone with the deleted promoter rescued all ASJ developmental defects of *tax-2(p691)* mutants. These data suggest that the phenotypes of *tax-2* are cell-autonomous in affected sensory neurons, since the *tax-2(p694)* deletion mutant should retain expression in ASJ (see above). Likewise, both *tax-2* clones that rescued the axon defects should be expressed in ASJ.

Defects were also observed in the ASE sensory neurons and the phasmid neurons. It was found that 45% of the ASE neurons in *tax-2(p691)* adults had both a

C

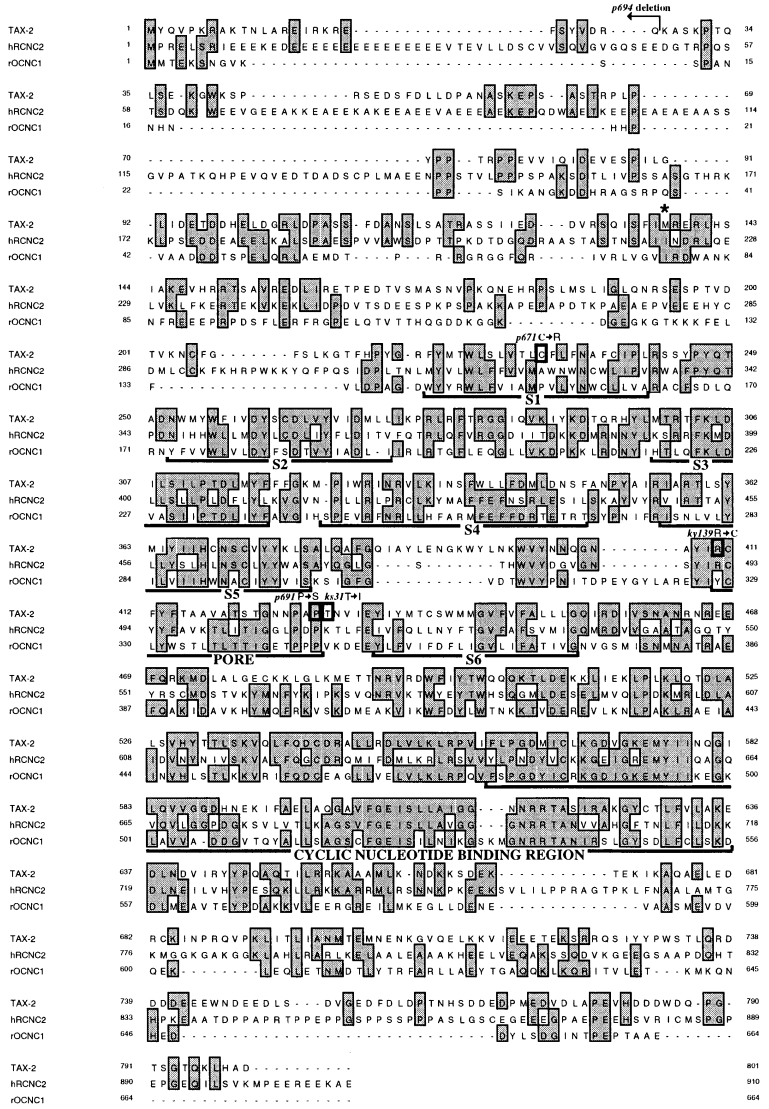

normal axon and an extra process that extended posteriorly from the ASE cell body (n = 204 animals). In 2%–6% of the mutant animals (depending on the mutant allele), the phasmid processes failed to terminate at the proper position in the ventral nerve cord. Mutant phasmid axons could continue in the ventral nerve cord for up to twice their normal length (Figures 4D and 4E). However, many of the sensory neurons appeared to have normal axons in *tax-2* and *tax-4* mutants. In particular, the AWC, AFD, and ASK axons were normal in the mutants, despite the compromised function of those sensory cell types (data not shown).

These results demonstrate that the cyclic nucleotide–gated channel affects both sensory function and outgrowth of some sensory cell axons. The timing of *tax-2* expression was consistent with functions in both development and transduction, since all *tax-2::GFP* fusion genes were expressed continuously from about midembryogenesis until the adult stage. Transduction molecules should be found in the sensory cilia, while guidance molecules should act in the axon. To explore these possibilities further, the location of the Tax-2 protein was examined using an epitope-tagged protein. The *tax-2* rescuing fragment was fused to the GFP at the 3′ end of the *tax-2* coding region (see Figure 2A). This Tax-2::GFP fusion gene fully rescued both the *tax-2* benzaldehyde chemotaxis defect (chemotaxis index = 0.90, n = 4 assays) and the axon guidance defect (98% normal axons by DiO staining, n = 165), indicating that the protein was functional.

Strong Tax-2::GFP protein expression was observed both in the sensory cilia and in the axons of the chemosensory neurons (see Figures 3C and 3D). Weaker fluorescence was visible in the dendrites and cell bodies. Tax-2::GFP was distributed similarly in *tax-4* mutants, but a Tax-2::GFP protein bearing the *p691* point muta-

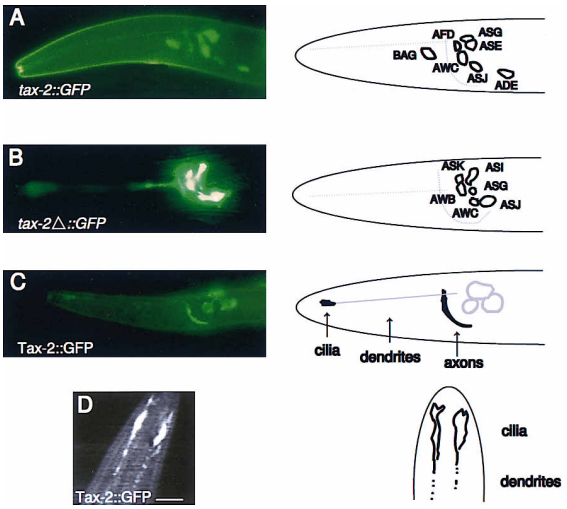

Figure 3. *tax-2* Protein Is Expressed in Sensory Neurons and Is Localized to Both the Sensory Cilia and the Axons

(A) GFP expression driven by the *tax-2::GFP* construct, which includes the upstream sequences and the first intron (see Figure 2C). Left-lateral view of a transgenic worm showing the GFP-expressing AWC, AFD, ASE, ASG, ASJ, ADE, and BAG neurons. The GFP-expressing ASK, ASI, and AWB neurons are out of this plane of focus. A construct that contained only the upstream sequences drove GFP expression in the neurons AWC, AFD, ASE, ASI, ADE, BAG, and occasionally ASK (data not shown). All constructs were expressed occasionally in the tail sensory neuron PQR; a phasmid neuron (PHA or PHB) was also seen rarely. Anterior is to the left, and dorsal is up.

(B) GFP expression driven by the *tax-2△::GFP* construct, which lacks the promoter and most of the first intron (mimicking the *tax-2(p694)* deletion; see Figure 2A). Left-lateral view of a transgenic worm showing the GFP-expressing neurons AWB, AWC, ASG, ASI, ASK, and ASJ. The positions of the sensory neurons are diagrammed at right. Anterior is to the left, and dorsal is up.

(C) Localization of the Tax-2::GFP tagged protein. Left-lateral view of a transgenic animal expressing the GFP-tagged Tax-2 protein. Intense staining in the sensory cilia and axons is diagrammed in black, while weaker staining in the dendrites and cell bodies is diagrammed in gray. Anterior is at left, and dorsal is up.

(D) Higher resolution view of Tax-2::GFP in the sensory cilia, generated by constrained iterative deconvolution. Dorsal view of the two bilaterally symmetrical AWC sensory cilia showing expression of the tagged Tax-2 protein. Other sensory cilia are out of the plane of focus. Anterior is at the top. Diagrammed dots indicate punctate staining in the dendrites. Scale bar, 5 μm.

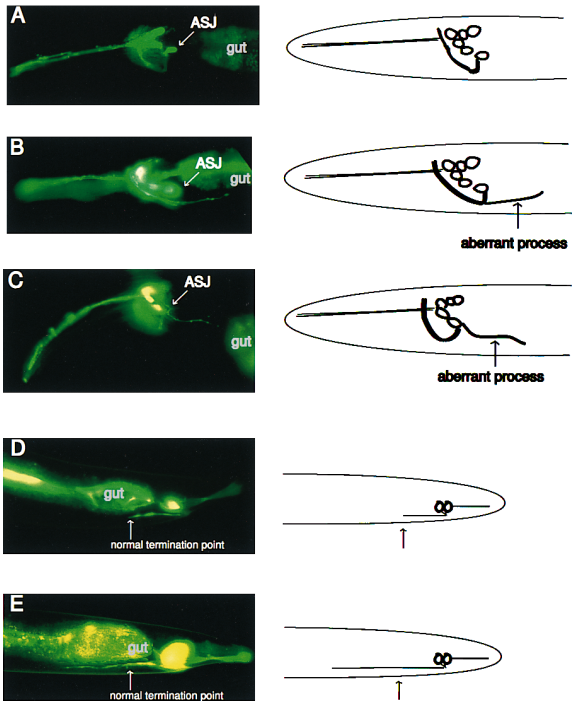

Figure 4. Developmental Defects of *tax-2* and *tax-4* Mutants Visualized by DiO Staining

(A) DiO staining of wild-type adult animal. Left-lateral view of one amphid showing dendrites, cell bodies, and axons of six amphid neurons. The normal position of the neuron ASJ is marked in (A)–(C). Some DiO staining is observed in the gut. In all cases, anterior is to the left and dorsal is up. Positions of the staining neurons are diagrammed.

(B) Left-lateral view of a DiO-stained *tax-2* mutant adult, showing an aberrant amphid neuron process projecting posteriorly from the nerve ring. *tax-4* animals have an identical phenotype.

(C) Left-lateral view of a DiO-stained *tax-2* mutant adult, showing an aberrant process projecting laterally from the ASJ neuron into the posterior body region. *tax-4* animals have an identical phenotype.

(D) DiO staining of wild-type phasmid neurons. Left-lateral view of one phasmid sensory organ showing dendrites, cell bodies, and axons of two phasmid sensory neurons. The normal termination point of the phasmid axons is marked.

(E) Left-lateral view of a *tax-2* mutant adult phasmid. The normal termination point of the phasmid axon is indicated. The *tax-4* mutant phenotype is identical.

tion was not localized to the cilia. These results indicate that localization to the cilia is sensitive to the structure of the Tax-2 protein, and likely to be specific, rather than nonspecific, protein sorting. In the axons, the Tax-2::GFP fusion protein was localized to the synapse-rich nerve ring and excluded from the amphid commissures, which lack synapses. The axon localization might be due to overexpression of the tagged protein; however, six GFP-tagged *odr-10* or *sr* receptors that are localized to the cilia are excluded from axons, even when they are expressed at comparably high levels (Sengupta et al., 1996; L. Tong, D. Tobin, E. Troemel, and C. I. B., unpublished data). The axon staining was visible as soon as Tax-2::GFP could be detected, at the comma stage of development when sensory axons form. Cilium staining was not visible until later in embryogenesis when cilia could be resolved (the pretzel stage).

tax-2 and *tax-4* May Function Together in Chemosensation and Axon Guidance

The similar mutant phenotypes of *tax-2* and *tax-4* suggested that they might function together as subunits of a single channel. To determine whether the *tax-2* and *tax-4* mutants showed any genetic interaction or redundancy, axon morphology and chemotaxis were observed in *tax-2; tax-4* double mutants. In all cases, *tax-2; tax-4* double mutant strains had similar phenotypes to the *tax-2* and *tax-4* single mutants, and no new defects were apparent (Figure 5). In particular, the same subset of olfactory responses was abnormal, and there was no increase in the number of defective axons per animal compared with the single mutants. This result indicates that the channel subunits are not redundant with one another to any appreciable extent; rather, they seem to act in a single process.

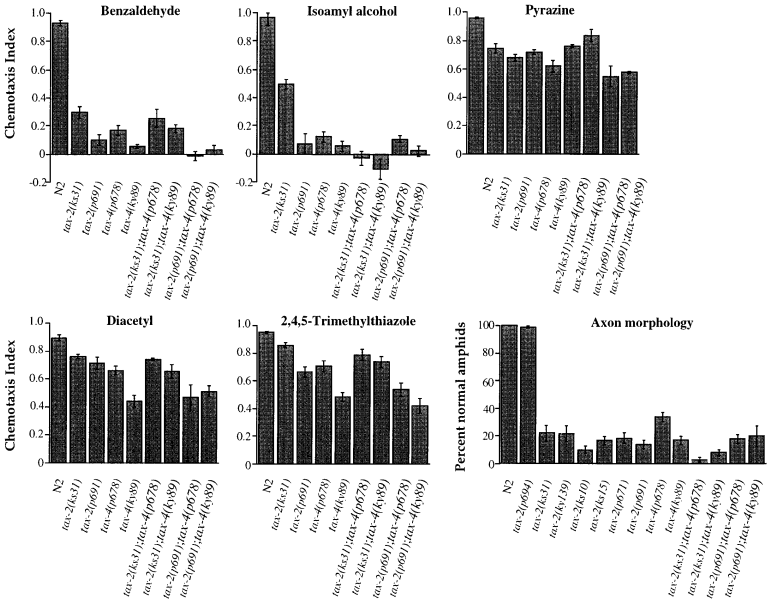

Figure 5. Chemotaxis and Axon Guidance Defects of *tax-2; tax-4* Double Mutants

For responses of *tax-2; tax-4* double mutant combinations to volatile odorants, each data point represents the average of 4–8 independent assays using ~100–200 animals per assay (error bars equal the SEM). The dilution of odorants in ethanol were the following: 1:200 benzaldehyde, 1:100 isoamyl alcohol, 10 mg/ml pyrazine, 1:1000 diacetyl, and 1:1000 2,4,5-trimethylthiazole. For amphid axon defects of *tax-2, tax-4,* and *tax-2; tax-4* double mutants, data points refer to the percentage of normal amphids (error bars denote the 95% confidence level). For each point, 200–700 DiO-stained adults were viewed; this assay reveals ASJ axons but not ASE axons. An amphid was scored as defective if any amphid neuron had a defect.

To ask whether either gene could compensate for the absence of the other, we injected the *tax-4* genomic rescuing clone into *tax-2* mutants, and vice versa. The transgenic animals generated in these experiments typically contain hundreds of copies of the transgene, and express 10–20 times as much protein as is expressed from the endogenous gene (Mello et al., 1991; A. V. Maricq and C. I. B, unpublished data). We found that high expression of *tax-4* was able to rescue both the chemotaxis phenotype and the axon guidance phenotype of *tax-2* mutants (Figure 6). Thus, an α-like cyclic nucleotide–gated channel gene can bypass defects in a β-like subunit when expressed at sufficiently high levels. The *tax-2* transgene did not ameliorate the *tax-4* mutant phenotype.

Discussion

A Predicted Cyclic Nucleotide–Gated Channel Acts in Olfaction, Salt Sensation, and Thermosensation

Cyclic nucleotide–gated channels are the major transduction channel in vertebrate olfactory neurons (Nakamura and Gold, 1987; Firestein et al., 1991). Our results implicate similar channels in C. elegans olfaction. Genetic characterization of *tax-2* and *tax-4* indicates that these two putative channel genes are essential for normal olfaction, and the Tax-2 protein is localized to the cilia where sensory transduction occurs. These observations suggest that similar channels are used in vertebrate and invertebrate olfaction. A Drosophila cyclic nucleotide–gated channel is expressed in the antennae, which contain fly olfactory neurons (Baumann et al., 1994); although its function is unknown, its localization is consistent with a role in olfaction.

While the AWC olfactory neurons require *tax-2* and *tax-4* function, the AWA olfactory neurons neither require nor express these two genes. Thus, different olfactory channels may operate in different olfactory cell types.

Interestingly, our results also implicate cyclic nucleotide–gated channels in salt taste and thermosensation. *tax-2* and *tax-4* mutants are defective in their ability to sense both Na^+ ions and Cl^- ions, and *tax-2* is expressed in the neurons that detect these ions (ASE) (Dusenbery et al., 1975; Bargmann and Horvitz, 1991a). In vertebrate salt sensation, an amiloride-sensitive sodium channel accounts for some, but not all, aspects of salt taste (Avenet and Lindemann, 1988), but the other components of this process are unknown. *tax-2* and *tax-4* mutants are also defective in thermotaxis and *tax-2* is expressed in the AFD thermosensory neurons, suggesting that the channel acts in thermosensation (Hedgecock and Russell, 1975; Mori and Ohshima, 1995). Little is known about thermotransduction; these results suggest that this sensory modality and many others share a common type of channel.

The Tax-2 and Tax-4 proteins have similar functions and appear to be expressed mostly in the same sensory neurons (Komatsu et al., 1996), suggesting that they might contribute to a single heteromeric channel. *tax-2* and *tax-4* mutants have similar behavioral and developmental defects, and *tax-2; tax-4* double mutants are indistinguishable from the single mutants. Since genetic and molecular results are consistent with the existing alleles being loss of function alleles, both subunits of the proposed C. elegans channel may be required for its function or proper regulation in vivo. Nonetheless, high levels of *tax-4* expression bypass the requirement for *tax-2,* suggesting that the α-like *tax-4* subunit can either function alone to a limited extent or provide some *tax-2* function. Similarly, while most vertebrate cyclic nucleotide–gated channels are probably heteromeric in vivo, the α subunits are capable of forming channels on their own when expressed at high levels (Kaupp et al., 1989; Dhallan et al., 1990). Beta subunits are required for the channels to show normal kinetics and nucleotide sensitivity (Chen et al., 1993; Bradley et al., 1994; Liman and Buck, 1994; Yao et al., 1995).

These genetic results demonstrate a requirement for

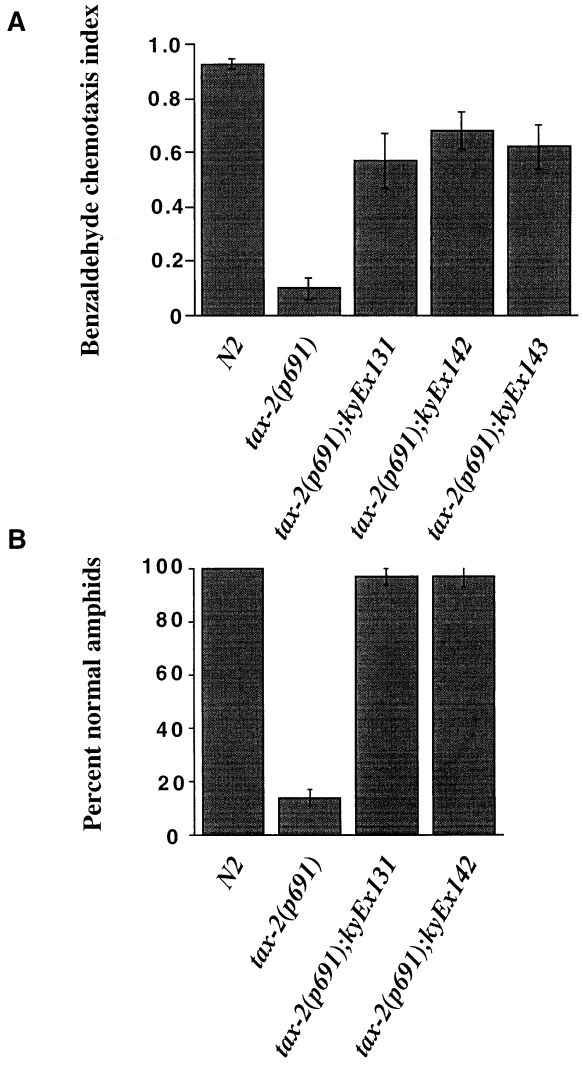

Figure 6. *tax-4* Overexpression Rescues *tax-2* Mutant Phenotypes

(A) Benzaldehyde chemotaxis of *tax-2(p691)* animals overexpressing *tax-4* genomic DNA. Each data point represents the average of eight to ten independent assays using ~100–200 animals per assay (error bars equal the SEM). *kyEx131, kyEx142, and kyEx143* are independent transgenic lines carrying extrachromosomal arrays of the *tax-4* rescuing clone and the coinjection marker. NaCl chemotaxis was also rescued in the transgenic strains (data not shown). Overexpression of p[*tax-2*] in *tax-4(p678)* did not rescue the *tax-4* chemotaxis phenotypes (data not shown).

(B) Amphid axon defects of *tax-2(p691)* animals overexpressing *tax-4* genomic DNA. Data points refer to the percentage of normal amphid axons (error bars equal the 95% confidence level). For each point, 200 DiO-stained adults were viewed. An amphid was scored as defective if any amphid neuron had a defect. Overexpression of the *tax-2* genomic DNA in *tax-4(p678)* did not rescue the *tax-4* amphid neuron defects (data not shown).

the channel in sensory neurons, but electrophysiological characterization will be required to demonstrate a direct role for the channel in transduction. By sequence, the *tax-2/tax-4* channel appears most likely to be cGMP activated, suggesting that it could respond to a phosphodiesterase cascade like that used in vertebrate vision (Stryer, 1991). However, it is possible that the channel plays a permissive or indirect role in function of the sensory neurons.

Axon Guidance and Termination Are Regulated by a Cyclic Nucleotide–Gated Channel

The *tax-2* and *tax-4* mutants reveal an unexpected function for the cyclic nucleotide–gated channel in the development of a few sensory neurons. C. elegans neurons have highly stereotyped axon morphologies in wild-type animals. In *tax-2* and *tax-4* mutants, the ASJ neurons frequently grow well beyond their normal stopping point, while the ASE neurons have an extra process in an ectopic location. Since the mutant axons are more extensive than wild-type axons, the normal activity of the channel inhibits or limits axon outgrowth in inappropriate regions.

Only a subset of the defective sensory neurons have abnormal axons in *tax-2* and *tax-4* mutants. In particular, the ASK, AWC, and AFD neurons, whose functions are essential for chemotaxis and thermotaxis, do not have any obvious developmental defects. Moreover, normal AWC olfactory behaviors can be generated when the *tax-2* gene product is provided only in the adult stage, consistent with a direct role of the channel in AWC olfaction rather than development (C. M. C., I. Mori, Y. Ohshima, C. I. B., unpublished data). We suggest that the channel functions primarily in sensory transduction, but has additional developmental effects in some neurons.

tax-2 and *tax-4* might have a permissive function in axon guidance, or they might mediate the recognition of instructive guidance cues. The cyclic nucleotide–gated channel could contribute to activity-dependent guidance of some axons. Although activity-dependent processes have not been previously described in C. elegans neuronal development, they drive a late stage of axon refinement in other sensory systems (Shatz and Stryker, 1988). However, the ASJ axon in *tax-2* and *tax-4* mutants is sometimes misrouted from the first point at which the axon leaves the cell body. This error occurs before normal sensory stimuli are present and before synapses are made, suggesting a function for the channel early in axon outgrowth. In addition, the presence of the Tax-2::GFP protein in the synaptic regions of sensory axons raises the possibility that the channel acts in axons to influence their outgrowth.

Indirect evidence from other systems suggests that cyclic nucleotides could function during the development of synapses. cGMP suppresses synapse formation at the vertebrate neuromuscular junction (Wang et al., 1995), and cAMP levels modify axon morphology in Aplysia and Drosophila (Zhong et al., 1992; Schacher et al., 1993). A vertebrate cyclic nucleotide–gated channel subunit is expressed on immature hippocampal neurites before synapses are formed (J. Bradley, Y. Zhang, and K. Zinn, personal communication). Cyclic nucleotide–gated channels might contribute to developmental functions by regulating calcium entry into cells (Frings et al., 1995). Mutations in several voltage-activated channels modify synaptic arbors of motor neurons in Drosophila (Budnik et al., 1990), and some in vitro models of neurite outgrowth depend on the activity of voltage-activated calcium channels (Williams et al., 1992).

During olfaction, it is likely that signal transduction is initiated through binding of ligands to seven transmembrane receptors such as the *sr* genes and *odr-10*-like genes (Troemel et al., 1995; Sengupta et al., 1996). The known receptors of this family appear to be localized

to the sensory cilia (Sengupta et al., 1996; L. Tong, D. Tobin, E. Troemel, and C. I. B., unpublished data). If *tax-2* and *tax-4* also act in the axons, different receptors might regulate the channel there. Axonal cGMP or cAMP could be produced by other G protein–coupled receptors, by ligand-activated transmembrane guanylyl cyclases, or by gases such as nitric oxide. A shared dependence on the *tax-2*/*tax-4* cyclic nucleotide–gated channel might allow cross-talk between sensory activity and connectivity of the neuron.

Experimental Procedures

Strain and Genetics

Wild-type worms were C. elegans variety Bristol, strain N2. Worms were grown on plates at 25°C, using standard methods (Brenner, 1974). The following strains were used in this work: PR691 *tax-2(p691)* I, PR671 *tax-2(p671)* I, PR694 *tax-2(p694)* I, CX139 *tax-2(ky139)* I, FK31 *tax-2(ks31)* I, FK10 *tax-2(ks10)* I, FK15 *tax-2(ks15)* I, PR678 *tax-4(p678)* III, and CX89 *tax-4(ky89)* III. Double mutant strains without additional marker mutations were constructed using standard genetic methods and verified by complementation testing.

Behavioral Assays

Population chemotaxis assays were performed as described (Bargmann et al., 1993). The chemotaxis index was defined as ($n_{attractant} - n_{counterattractant}$)/Total n. Osmotic avoidance assays were performed as described (Vowels and Thomas, 1994). Negative chemotaxis to 1-octanol and 2-nonanone was tested on square assay plates; in other respects, this population chemotaxis assay is similar to positive chemotaxis assays (B. E. Kimmel and C. I. B., unpublished data). Long-range negative chemotaxis is distinct from the acute reversal seen in response to a pulse of 1-octanol (Troemel et al., 1995).

DiO Staining and GFP Visualization of Chemosensory Neurons

DiO staining was performed essentially as described (Herman and Hedgecock, 1990), except that animals were stained for 16–18 hr on a rotator in the presence of 1 μl of concentrated Escherichia coli per ml of M9 buffer. Stained animals were viewed by fluorescence microscopy; only adults were scored, since DiO staining of larvae is variable. An animal was scored as having defective amphids if any amphid neuron had abnormal axons (see Figure 3). A set of GFP fusion genes was used to identify the affected DiO-staining neuron, and to visualize other sensory neurons (particularly AWC, AFD, ASE, and ASK). These included a *ceh-23::GFP* fusion gene, which stains AWC, AFD, ASE, ADF, ASG, ASH, and ADL neurons (Wang et al., 1993; J. Zallen and C. I. B., unpublished data), *M7::GFP* (ASI), and *C42::GFP* (AWB) (E. Troemel and C. I. B., unpublished data), and *tax-2::GFP* fusion genes (see below) including *tax-2Δ::GFP* (AWB, AWC, ASG, ASI, ASJ, and ASK) and *tax-2p::GFP* (AWC, AFD, ASE, ASI, ADE, BAG, and occasionally ASK). The *tax-2* fusion genes were visualized as unstable arrays, so that only a subset of cells stained in many animals, allowing matching of individual cells with affected axons. The ASE defects observed with *tax-2p::GFP* were apparent in all four larval stages and the adult, whereas ASJ defects observed with *tax-2Δ::GFP* were only apparent in L4 and adult stages. High resolution three-dimensional images of Tax-2::GFP protein in the cilia were acquired using wide-field fluorescence microscopy and refined by constrained iterative deconvolution (Hiraoka et al., 1990).

Molecular Biology Methods

General DNA manipulations were carried out as described (Sambrook et al., 1989). Nested deletions for DNA sequencing were generated using Exonuclease III (New England Biolabs) and sequenced using the *fmol* sequencing system (Promega). Sequence analysis was performed using Geneworks (Intelligenetics). Sequence comparisons were carried out using the BLAST network service (Altschul et al., 1990), and sequence alignments were produced using the CLUSTAL W program (Thompson et al., 1994).

Germline Transformation

Germline transformation (Mello et al., 1991) was performed by coinjecting test DNA at a concentration of 10–40 μg/ml and marker DNA at a concentration of 60 μg/ml into the gonad of animals. For *tax-2* injections, the *tax-2(p691)* strain was injected with *glr-1::GFP* marker DNA (Maricq et al., 1995) and transgenic animals were recognized on the basis of neuronal GFP expression. For *tax-4* injections, a *tax-4; lin-15(n765ts)* strain was injected with JM23 *lin-15* marker DNA, and transgenic animals were recognized by rescue of the *lin-15* multivulval phenotype at 20°C (Huang et al., 1994). Multiple independent lines were established from each injection.

Genomic Localization of *tax-2*

tax-2 had been incorrectly mapped to chromosome II, but we found that *p691* was linked to chromosome I, between the two cloned genes *unc-29* and *lin-11*; from a strain of genotype *tax-2/unc-29 lin-11*, 3/15 Lin non-Unc recombinants segregated *tax-2* and 57/60 Unc non-Lin segregated *tax-2.* Cosmid clones from this interval were tested for their ability to complement the *tax-2* mutant phenotype in transgenic worms. The cosmid T18D4 rescued the *tax-2(p691)* benzaldehyde chemotaxis defect and the axon outgrowth phenotype, as did a 6.5 kb HindIII fragment of T18D4. The 6.5 kb fragment was sequenced on one strand, revealing one open reading frame. A frame-shift mutation was introduced into the 6.5 kb HindIII fragment by digesting with BsaB1 and inserting a linker with the sequence 5′-CCCCCGGGGG-3′ (New England BioLabs). This insertion added eight amino acids after position 384 followed by a stop codon at position 393, effectively deleting transmembrane domains 4 and 5, the presumed pore and cyclic nucleotide–binding regions and the COOH-terminus. This construct failed to rescue the *tax-2(p691)* mutant phenotypes. A genomic clone containing the entire coding region of *tax-2* plus 1.8 kb of upstream sequences was constructed by adding a 2.2 kb BglI–HindIII fragment 5′ to the 6.5 kb HindIII fragment.

Isolation and Characterization of cDNAs

The 6.5 kb HindIII genomic fragment was used to screen approximately 1.1×10^6 plaques of a mixed-stage worm cDNA library (Barstead and Waterston, 1989). Three positive clones were identified, and DNA sequencing revealed that they were overlapping partial cDNAs beginning at amino acid positions 399, 492, and 527 and continuing to the 3′ end. RT–PCR was used to isolate the remainder of the cDNA. Total worm RNA was prepared from mixed-stage N2 worms by LiCl precipitation (M. Finney, personal communication). First-strand cDNA was synthesized using an oligonucleotide in exon 8 and was used as a template for subsequent amplification using nested oligonucleotides. The conditions used for PCR were the following: 30 s at 95°C, 1 min at 52°C, and 2 min at 72°C for 30 or 35 cycles followed by 10 min at 72°C. One band of 661 bp was detected and sequenced. In a second experiment, first-strand cDNA was synthesized using an oligonucleotide in exon 4 and was used as a template for subsequent amplification using oligonucleotides that detect SL-1 and SL-2 *trans*-spliced mRNAs (Huang and Hirsh, 1989). Reactions were subjected to additional rounds of amplification using nested oligonucleotides. A 704 bp band was detected in samples amplified using SL-1. No bands were detected in reactions using SL-2. All cDNAs were sequenced on both strands.

Sequencing of *tax-2* Alleles

Genomic DNA was isolated from *N2*, *tax-2(p694)*, *tax-2(p671)*, *tax-2(p691)*, *tax-2(ks10)*, *tax-2(ks15)*, *tax-2(ks31)*, and *tax-2(ky139)* worms as described (Klein and Meyer, 1993). Fragments of *tax-2* genomic DNA were PCR-amplified using primers within introns and sequenced using ^{33}P end-labeled primers. At least one strand of the open reading frame of all 14 exons, their splice junctions, and ~30 bp beyond the 3′ and 5′ ends of open reading frames were sequenced. The exons containing the mutations were sequenced on both strands. PCR and Southern blot analysis of N2 and *tax-2(p694)* genomic DNA revealed an ~2 kb deletion encompassing exon 1 and ~1.6 kb 5′ of the *tax-2* coding region. To define the right breakpoint of the deletion, primers flanking this region were used to amplify and sequence the region from *tax-2(p694)*.

tax-2::GFP Expression

Translational fusions between *tax-2* and GFP were constructed using expression vectors provided by A. Fire (A. Fire, S. Xu, J. Ahnn, and G. Seydoux, personal communication). The *tax-2* promoter construct was constructed by amplifying 1.8 kb of *tax-2* upstream sequence and the first three amino acids of *tax-2* from genomic DNA, using the Expand PCR kit (Boehringer Mannheim). The conditions used for PCR were the following: 30 s at 95°C, 1 min at 52°C, and 2 min at 72°C for 20 cycles, followed by 10 min at 72°C. This fragment was digested with BamHI and SalI and ligated into the GFP expression vector pPD95.79 to make P[*tax-2p::GFP*]. To make P[*tax-2::GFP*], the BglI–SalI genomic fragment containing ~1.8 kb of *tax-2* upstream sequences and 215 amino acids of *tax-2* protein was ligated into the GFP expression vector pPD95.77. To make P[*tax-2Δ::GFP*], the HindIII–SalI genomic fragment containing part of intron 1 and 188 amino acids of *tax-2* coding region was ligated into pPD95.77. Constructs were coinjected with plasmid pJM23(*lin-15*) into the gonads of *lin-15(n765ts)* animals and *lin-15(+)*-transformed progeny were viewed using fluorescence microscopy.

The GFP-tagged Tax-2 protein was constructed by ligating the 4.2 kb HindIII–BamHI genomic fragment into the GFP expression vector pPD95.75. This construct was injected into *lin-15(n765ts)* animals with pJM23 as described above. The Tax-2 GFP-tagged gene was also injected into *tax-2(p691)* animals using *glr-1::GFP* coinjection marker, and GFP-positive transformed progeny were assayed for rescue of *tax-2* mutant phenotypes.

Expression of *tax-4* in *tax-2* Mutants

The *tax-4* genomic rescuing clone pSF12 (Komatsu et al., 1996) and coinjection marker *glr-1::GFP* were injected into *tax-2(p691)* mutant worms. The *tax-2* full-length genomic rescuing clone was injected into *tax-4(n678); lin-15(n765)* mutant worms with pJM23. Transgenic strains were identified by GFP fluorescence or rescue of the *lin-15* multivulval phenotype, respectively.

Generating the *tax-2(p691)* Mutant Allele

To ask whether *tax-2* mutations poison wild-type *tax-4* function, the *tax-2(p691)* mutant allele was injected into wild-type animals. These animals responded normally to odorants and had normal sensory axons, indicating that the transgene did not disrupt the function of the endogenous *tax-2* and *tax-4* genes. PCR was used to amplify the full *tax-2* coding region and about 1.8 kb of upstream sequences from *tax-2(p691)* genomic DNA, using the Expand kit (Boehringer Mannheim). The conditions used for PCR were the following: 30 s at 95°C, 1 min at 54°C, and 8 min at 72°C for 30 or 35 cycles followed by 10 min at 72°C. The 6.4 kb fragment was gel purified using Gene Clean (Bio101) and injected into *lin-15(n765ts)* animals with pJM23. Transformed progeny were assayed for chemotaxis and axon outgrowth phenotypes. A smaller amplified fragment of *p691* was used to construct a GFP-tagged Tax-2 protein bearing the mutation.

Acknowledgments

We thank Ikue Mori for stimulating discussions and for sharing her data with us prior to publication, Wallace Marshall for generating the high magnification image of Tax-2::GFP protein, Didier Stainier, Lily Jan, Cynthia Kenyon, Marc Tessier-Lavigne, Jen Zallen, David Tobin, and Noelle Dwyer for their comments on this manuscript, Kate Wesseling, Shannon Grantner, and Liqin Tong for excellent technical support, Amy Kistler for isolating *ky89*, Kent Nybakken, Hernan Espinoza, and Emily Troemel for characterization of some *tax-2* alleles, and Andrew Fire for the expression vectors. Some strains were provided by the Caenorhabditis Genetics Center. This work was supported by National Institutes of Health grant DC01393 and funds from the Lucille P. Markey Trust and the Searle Scholars Program; C. M. C. was supported by a predoctoral fellowship from the National Science Foundation; C. I. B. is an Assistant Investigator of the Howard Hughes Medical Institute.

The costs of publication of this article were defrayed in part by the payment of page charges. This article must therefore be hereby marked *"advertisement"* in accordance with 18 USC Section 1734 solely to indicate this fact.

Received July 23, 1996; revised September 17, 1996.

References

Ahmad, I., Leinders-Zufall, T., Kocsis, J.D., Shepherd, G.M., Zufall, F., and Barnstable, C.J. (1994). Retinal ganglion cells express a cGMP-gated cation conductance activatable by nitric oxide donors. Neuron *12*, 155–165.

Altschul, S.F., Gish, W., Miller, W., Myers, E.W., and Lipman, D.J. (1990). Basic local alignment search tool. J. Mol. Biol. *215*, 403–410.

Avenet, P., and Lindemann, B. (1988). Amiloride-blockable sodium currents in isolated taste receptor cells. J. Memb. Biol. *105*, 245–255.

Bargmann, C.I., and Horvitz, H.R. (1991a). Chemosensory neurons with overlapping functions direct chemotaxis to multiple chemicals in C. elegans. Neuron *7*, 729–742.

Bargmann, C.I., and Horvitz, H.R. (1991b). Control of larval development by chemosensory neurons in *Caenorhabditis elegans*. Science *251*, 1243–1246.

Bargmann, C.I., Hartwieg, E., and Horvitz, H.R. (1993). Odorant-selective genes and neurons mediate olfaction in *C. elegans*. Cell *74*, 515–527.

Barstead, R.J., and Waterston, R.H. (1989). The basal component of the nematode dense-body is vinculin. J. Biol. Chem. *264*, 10177–10185.

Baumann, A., Frings, S., Godde, M., Seifert, R., and Kaupp, U.B. (1994). Primary structure and functional expression of a Drosophila cyclic nucleotide–gated channel present in eyes and antennae. EMBO J. *13*, 5040–5050.

Biel, M., Zong, X., Distler, M., Bosse, E., Klugbauer, N., Murakami, M., Flockerzi, V., and Hofmann, F. (1994). Another member of the cyclic nucleotide–gated channel family, expressed in testis, kidney, and heart. Proc. Natl. Acad. Sci. USA *91*, 3505–3509.

Bonigk, W., Altenhofen, W., Muller, F., Dose, A., Illing, M., Molday, R.S., and Kaupp, U.B. (1993). Rod and cone photoreceptor cells express distinct genes for cGMP-gated channels. Neuron *10*, 865–877.

Bradley, J., Li, J., Davidson, N., Lester, H.A., and Zinn, K. (1994). Heteromeric olfactory cyclic nucleotide–gated channels: a new subunit that confers increased sensitivity to cAMP. Proc. Natl. Acad. Sci. USA *91*, 8890–8894.

Brenner, S. (1974). The genetics of Caenorhabditis elegans. Genetics *77*, 71–94.

Budnik, V., Zhong, Y., and Wu, C.F. (1990). Morphological plasticity of motor axons in Drosophila mutants with altered excitability. J. Neurosci. *10*, 3754–3768.

Chen, T.-Y., Peng, Y.-W., Dhallan, R.S., Ahamed, B., Reed, R.R., and Yau, K.-W. (1993). A new subunit of the cyclic nucleotide–gated cation channel in retinal rods. Nature *362*, 764–767.

Colbert, H.A., and Bargmann, C.I. (1995). Odorant-specific adaptation pathways generate olfactory plasticity in *C. elegans*. Neuron *14*, 803–812.

Dhallan, R.S., Yau, K.-W., Schrader, K.A., and Reed, R.R. (1990). Primary structure and functional expression of a cyclic nucleotide–activated channel from olfactory neurons. Nature *347*, 184–187.

Dubin, A.E., and Dionne, V.E. (1994). Action potentials and chemosensitive conductances in the dendrites of olfactory neurons suggest new features for odor transduction. J. Gen. Physiol. *103*, 181–201.

Dusenbery, D.B., Sheridan, R.E., and Russell, R.L. (1975). Chemotaxis-defective mutants of the nematode Caenorhabditis elegans. Genetics *80*, 297–309.

el-Husseini, A.e.-D., Bladen, C., and Vincent, S.R. (1995). Expression of the olfactory cyclic nucleotide gated channel (CNG1) in the rat brain. Neuroreport *6*, 1459–1463.

Felsenfeld, J. (1989). PHYLIP—Phylogeny Inference Program (Version 3.2). Cladistics *5*, 164–166.

Fesenko, E., Kolesnikov, S., and Lyubarsky, A. (1985). Induction by cGMP of cationic conductance in plasma membrane of retinal rod outer segment. Nature *313*, 310–313.

Firestein, S., Zufall, F., and Shepherd, G.M. (1991). Single odor-sensitive channels in olfactory receptor neurons are also gated by cyclic nucleotides. J. Neurosci. *11*, 3565–3572.

Frings, S., Seifert, R., Godde, M., and Kaupp, U.B. (1995). Profoundly different calcium permeation and blockage determine the specific function of distinct cyclic nucleotide–gated channels. Neuron *15*, 169–179.

Goulding, E.H., Tibbs, G.R., and Siegelbaum, S.A. (1994). Molecular mechanism of cyclic nucleotide–gated channel activation. Nature *372*, 369–374.

Hedgecock, E.M., and Russell, R.L. (1975). Normal and mutant thermotaxis in the nematode Caenorhabditis elegans. Proc. Natl. Acad. Sci. USA *72,* 4061–4065.

Henn, D.K., Baumann, A., and Kaupp, U.B. (1995). Probing the transmembrane topology of cyclic nucleotide–gated ion channels with a gene fusion approach. Proc. Natl. Acad. Sci. USA *92*, 7425–7429.

Herman, R., and Hedgecock, E. (1990). Limitation of the size of the vulval primordium of Caenorhabditis elegans by lin-15 expression in surrounding hypodermis. Nature *348*, 169–171.

Hiraoka, Y., Sedat, J.W., and Agard, D.A. (1990). Determination of three-dimensional imaging properties of a light microscope system. Partial confocal behavior in epifluorescence microscopy. Biophys. J. *57*, 325–333.

Huang, L.S., Tzou, P., and Sternberg, P.W. (1994). The lin-15 locus encodes two negative regulators of Caenorhabditis elegans vulval development. Mol. Biol. Cell *5*, 395–412.

Huang, X.Y., and Hirsh, D. (1989). A second trans-spliced RNA leader sequence in the nematode Caenorhabditis elegans. Proc. Natl. Acad. Sci. USA *86*, 8640–8644.

Kaplan, J., and Horvitz, H. (1993). A dual mechanosensory and chemosensory neuron in *Caenorhabditis elegans*. Proc. Natl. Acad. Sci. USA *90*, 2227–2231.

Kaupp, U., Nudome, T., Tanabe, T., Terada, S., Bonigk, W., Stuhmer, W., Cook, N., Kangawa, K., Matsuo, H., Hirose, T., Miyata, T., and Numa, S. (1989). Primary structure and functional expression of complementary DNA of the rod photoreceptor cyclic GMP-gated channel. Nature *342*, 762–766.

Kleene, S.J. (1993). Origin of the chloride current in olfactory transduction. Neuron *11*, 123–132.

Klein, R.D., and Meyer, B.J. (1993). Independent domains of the Sdc-3 protein control sex determination and dosage compensation in C. elegans. Cell *72*, 349–364.

Komatsu, H., Mori, I., Rhee, J.-S., Akaike, N., and Ohshima, Y. (1996). Mutations in a cyclic nucleotide–gated channel lead to abnormal thermosensation and chemosensation in C. elegans. Neuron *17*, this issue.

Korschen, H.G., Illing, M., Seifert, R., Sesti, F., Williams, A., Gotzes, S., Colville, C., Muller, F., Dose, A., Godde, M., Molday, L., Kaupp, U.B., and Molday, R.S. (1995). A 240 kDa protein represents the complete β subunit of the cyclic nucleotide–gated channel from rod photoreceptor. Neuron *15*, 627–636.

Lewis, J.A., and Hodgkin, J.A. (1977). Specific neuroanatomical changes in chemosensory mutants of the nematode Caenorhabditis elegans. J. Comp. Neurol. *172*, 489–510.

Liman, E.R., and Buck, L.B. (1994). A second subunit of the olfactory cyclic nucleotide–gated channel confers high sensitivity to cAMP. Neuron *13*, 611–621.

Lowe, G., and Gold, G.H. (1993). Nonlinear amplification by calcium-dependent chloride channels in olfactory receptor cells. Nature *366*, 283–286.

Maricq, A.V., Peckol, E., Driscoll, M., and Bargmann, C.I. (1995). Mechanosensory signaling in *C. elegans* mediated by the GLR-1 glutamate receptor. Nature *378*, 78–81.

Mello, C.C., Kramer, J.M., Stinchcomb, D., and Ambros, V. (1991). Efficient gene transfer in C. elegans: extrachromosomal maintenance and integration of transforming sequences. EMBO J. *10*, 3959–3970.

Mori, I., and Ohshima, Y. (1995). Neural regulation of thermotaxis in Caenorhabditis elegans. Nature *376*, 344–348.

Nakamura, T., and Gold, G.H. (1987). A cyclic-nucleotide gated conductance in olfactory receptor cilia. Nature *325*, 442–444.

Sambrook, J., Fritsch, E.F., and Maniatis, T. (1989). Molecular Cloning: A Laboratory Manual (Cold Spring Harbor, New York: Cold Spring Harbor Press).

Schacher, S., Kandel, E.R., and Montarolo, P. (1993). cAMP and arachidonic acid simulate long-term structural and functional changes produced by neurotransmitters in Aplysia sensory neurons. Neuron *10*, 1079–1088.

Sengupta, P., Chou, J.C., and Bargmann, C.I. (1996). *odr-10* encodes a seven transmembrane domain olfactory receptor required for responses to the odorant diacetyl. Cell *84*, 899–909.

Shatz, C., and Stryker, M. (1988). Prenatal tetrodotoxin infusion blocks segregation of retinogeniculate afferents. Science *242*, 87–89.

Sklar, P.B., Anholt, R.R.H., and Snyder, S.H. (1986). The odorant-sensitive adenylate cyclase of olfactory receptor cells: differential stimulation by distinct classes of odorants. J. Biol. Chem. *261*, 25538–25543.

Stryer, L. (1991). Visual excitation and recovery. J. Biol. Chem. *266*, 10711–10714.

Thompson, J.D., Higgins, D.G., and Gibson, T.J. (1994). CLUSTAL W: improving the sensitivity of progressive multiple sequence alignment through sequence weighting, position-specific gap penalties and weight matrix choice. Nucl. Acids Res. *22*, 4673–4680.

Troemel, E.R., Chou, J.H., Dwyer, N.D., Colbert, H.A., and Bargmann, C.I. (1995). Divergent seven transmembrane receptors are candidate chemosensory receptors in C. elegans. Cell *83*, 207–218.

Varnum, M.D., Black, K.D., and Zagotta, W.N. (1995). Molecular mechanism for ligand discrimination of cyclic nucleotide–gated channels. Neuron *15*, 619–625.

Vowels, J., and Thomas, J. (1994). Multiple chemosensory defects in *daf-11* and *daf-21* mutants of Caenorhabditis elegans. Genetics *138*, 303–316.

Wang, B.B., Muller-Immergluck, M.M., Austin, J., Robinson, N.T., Chisholm, A., and Kenyon, C. (1993). A homeotic gene cluster patterns the anteroposterior body axis of C. elegans. Cell *74*, 29–42.

Wang, T., Xie, Z., and Lu, B. (1995). Nitric oxide mediates activity-dependent synaptic suppression at developing neuromuscular synapses. Nature *374*, 262–266.

Ward, S. (1973). Chemotaxis by the nematode Caenorhabditis elegans: identification of attractants and analysis of the response by use of mutants. Proc. Natl. Acad. Sci. USA *70*, 817–821.

Ward, S., Thomson, N., White, J.G., and Brenner, S. (1975). Electron microscopical reconstruction of the anterior sensory anatomy of the nematode Caenorhabditis elegans. J. Comp. Neurol. *160*, 313–337.

Ware, R.W., Clark, D., Crossland, K., and Russell, R.L. (1975). The nerve ring of the nematode *Caenorhabditis elegans*: sensory input and motor output. J. Comp. Neurol. *162*, 71–110.

Weyand, I., Godde, M., Frings, S., Weiner, J., Muller, F., Altenhofen, W., Hatt, H., and Kaupp, U.B. (1994). Cloning and functional expression of a cyclic-nucleotide–gated channel from mammalian sperm. Nature *368*, 859–863.

White, J.G., Southgate, E., Thomson, J.N., and Brenner, S. (1986). The structure of the nervous system of the nematode *Caenorhabditis elegans*. Phil. Trans. R. Soc. Lond. B *314*, 1–340.

Williams, E.J., Doherty, P., Turner, G., Reid, R.A., Hemperly, J.J., and Walsh, F.S. (1992). Calcium influx into neurons can solely account for cell contact-dependent neurite outgrowth stimulated by transfected L1. J. Cell Biol. *119*, 883–892.

Yao, X., Segal, A.S., Welling, P., Zhang, X., McNicholas, C.M., Engel, D., Boulpaep, E.L., and Desir, G.V. (1995). Primary structure and

functional expression of a cGMP-gated potassium channel. Proc. Natl. Acad. Sci. USA *92*, 11711–11715.

Zhong, Y., Budnik, V., and Wu, C.F. (1992). Synaptic plasticity in Drosophila memory and hyperexcitable mutants: role of cAMP cascade. J. Neurosci. *12*, 644–651.

GenBank Accession Number

The accession number for the *tax-2* gene reported in this paper is U73476.